

Inclusive Higgs boson cross-section for the LHC at 8 TeV

Charalampos Anastasiou

Institute for Theoretical Physics, ETH Zurich, 8093 Zurich, Switzerland
E-mail: babis@phys.ethz.ch

Stephan Buehler

Institute for Theoretical Physics, ETH Zurich, 8093 Zurich, Switzerland
E-mail: buehler@itp.phys.ethz.ch

Franz Herzog

Institute for Theoretical Physics, ETH Zurich, 8093 Zurich, Switzerland
E-mail: fhertzog@itp.phys.ethz.ch

Achilleas Lazopoulos

Institute for Theoretical Physics, ETH Zurich, 8093 Zurich, Switzerland
E-mail: lazopoli@itp.phys.ethz.ch

ABSTRACT: We present the inclusive Higgs boson cross-section at the LHC with collision energy of 8 TeV. Our predictions are obtained using our publicly available program `iHixs` which incorporates NNLO QCD corrections and electroweak corrections. We review the convergence of the QCD perturbative expansion at this new energy and examine the impact of finite Higgs width effects. We also study the impact of different parton distribution functions on the cross-section. We present tables with the cross-section values and estimates for their uncertainty due to uncalculated higher orders in the perturbative expansion and parton densities.

KEYWORDS: QCD, NLO, NNLO, LHC.

1. Introduction

Experiments at the Large Hadron Collider have made an impressive progress in the search for the Higgs boson during 2011. In the Standard Model, only a small window of Higgs boson masses is in agreement with LHC [1,2], Tevatron [3] and LEP [4] data. The search for the Higgs boson will resume shortly in 2012. A discovery or exclusion of a Standard Model Higgs is eminent, provided of course that the theoretical prediction is solid and that the LHC machine and experiments perform as anticipated. In 2012, proton-proton collisions at the LHC will have a new center of mass energy of 8 TeV.

The purpose of this article is to provide numerical results for the inclusive gluon fusion Higgs boson cross-section at 8 TeV. We obtain state of the art predictions for the inclusive gluon fusion cross section and its uncertainties with our publicly available computer program *iHixs* [5]. *iHixs* evaluates the contribution to the cross-section in NNLO QCD and includes important electroweak effects. A detailed description of the theoretical contributions [6–20] which are incorporated and accounted for in *iHixs* can be found in the corresponding publication [5].

In Section 2 we study the convergence of the perturbative QCD corrections. In Section 3 we study the sensitivity of the cross-section on parton densities. In Section 4 we study the effect of the Higgs width. In Section 6 we present our numerical values for the cross-section and its uncertainties.

2. Perturbative convergence and scale uncertainties

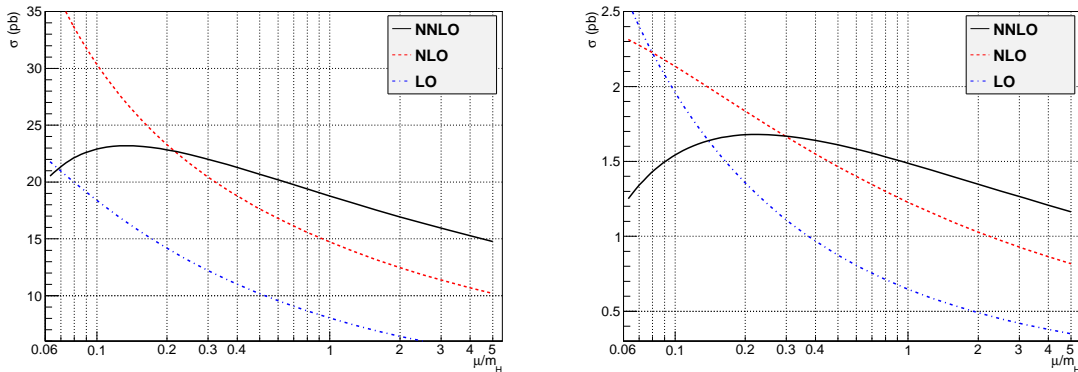


Figure 1: Scale dependence of the gluon fusion cross-section at LO, NLO, and NNLO for $m_H = 125$ GeV (left panel) and $m_H = 450$ GeV (right panel). The perturbative series converges faster for scale choices smaller than Higgs boson mass.

The perturbative convergence of the Higgs boson cross-section has been studied thoroughly during the last decade. We find a similar convergence pattern at the new LHC energy of 8 TeV as for 7 TeV and 14 TeV. For illustration, we present in Figure 2 the behavior of the cross-section at 8 TeV by varying the renormalization and factorization

scales $\mu = \mu_R = \mu_F$ simultaneously¹. As it has already been realized in the literature, smaller scales than the Higgs boson mass lead to a faster convergence of the perturbative expansion [5, 6].

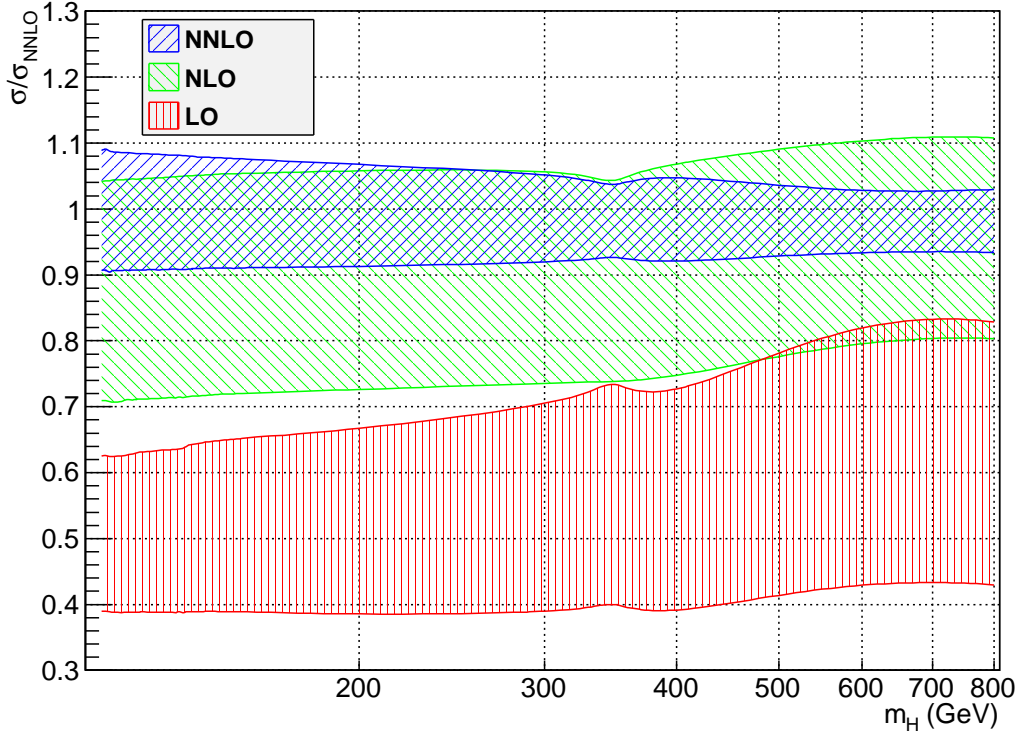


Figure 2: Scale variation of the gluon fusion cross-section at LO, NLO, and NNLO. The LO, NLO and NNLO cross-sections at scale $\mu \in [\frac{m_H}{4}, m_H]$ are normalized to the NNLO cross-section at the central scale $\mu = \frac{m_H}{2}$.

We estimate the theoretical uncertainty from uncalculated higher order corrections by varying the renormalization and factorization scale in the interval $\mu \in [\frac{m_H}{4}, m_H]$. In Fig 2 we present the cross-section at LO, NLO and NNLO in this interval, normalized to the NNLO cross-section at the central scale $\mu = \frac{m_H}{2}$. The NNLO and NLO bands overlap largely. Corrections beyond NNLO would need to be atypical in order for our uncertainty estimate to be inaccurate. The cross-section is known to be stable under threshold and other corrections which can be resummed beyond NNLO [23–25].

3. Parton density function comparison

The Higgs boson cross-section requires parton distribution functions (pdf) as input. In `iHixs` we employ all pdf sets that allow for NNLO evolution (MSTW08 [27], JR09 [28], NNPDF

¹We use the central MSTW08 PDF set for all results in this section.

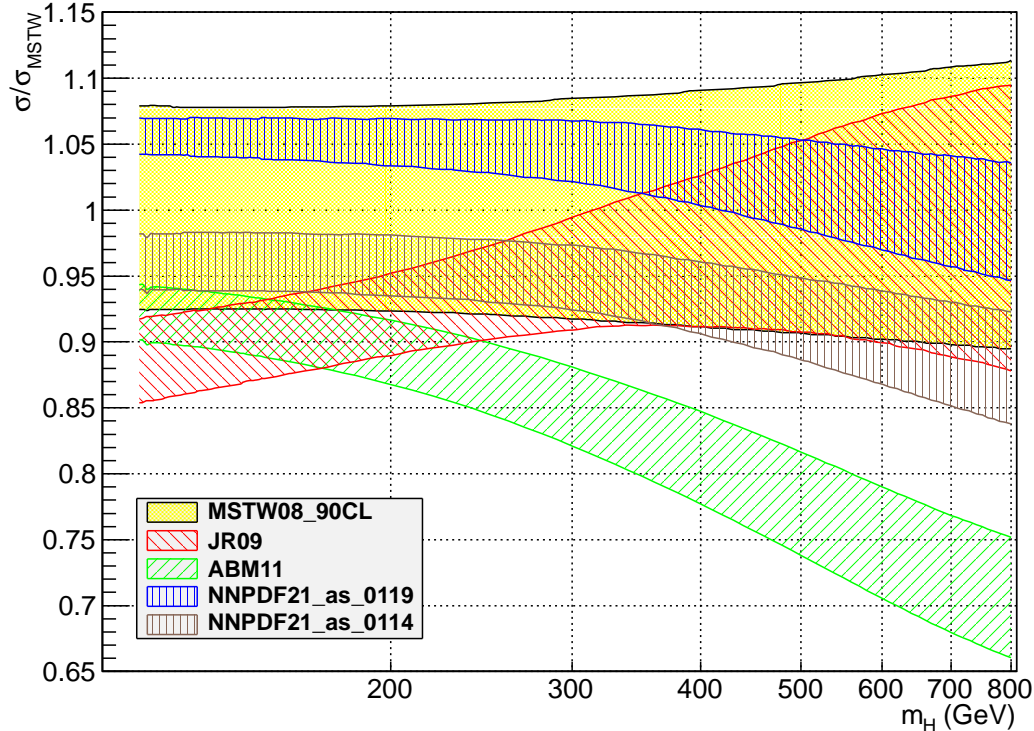


Figure 3: The uncertainty of the Higgs cross-section due to the parton distribution functions.

[29], ABM11 [30]) and are publicly available through the LHAPDF [17, 26] library.

Our knowledge of the parton densities has been increasing steadily over the recent years. The gluon density is being extracted with an accuracy of a few percent over a large range of Bjorken- x values. However, a direct comparison exposes differences beyond the quoted uncertainties. These discrepancies affect the gluon density and the fitted value of α_s which are very important input for the calculation of the Higgs boson cross-section.

In Figure 3 we present uncertainty bands for each pdf provider, normalizing all cross-sections to the central value of the NNLO MSTW08 set. The MSTW uncertainty band is at 90% confidence level². The uncertainties of the other pdf sets are at 68% confidence level. For the NNPDF set we present the Higgs cross-section for the nominal value of the strong coupling $\alpha_s = 0.119$ and for the lowest value $\alpha_s = 0.114$ for which a set is provided. This value is close to that extracted by the ABM11 group and shows that the discrepancy between the two sets cannot be attributed entirely to the value of a_s .

The differences of pdf sets beyond their quoted uncertainties has been a tantalizing issue. The discrepancies between the MSTW and NNPDF pdf sets (and in the high mass region, also the JR set) can be partially accounted for by enlarging the uncertainty of the

²The 68% confidence level uncertainty reduces the width of the band to about half, as it is anticipated by a naive error propagation of the gluon density uncertainty to the gluon partonic luminosity

MSTW08 set to the one obtained at 90% confidence level. We will therefore use MSTW08 at 90%CL as our main benchmark set.

The discrepancy between the ABM11 and the other sets is large and becomes rather dramatic for high values of the Higgs boson mass. Notably, the ABM11 set finds a value of $\alpha_s = 0.1134(11)$ which is quite small in comparison to the world average ($\alpha_s = 0.1184(7)$) [31]. It is alarming to us that the extractions of α_s based on quantities which are known precisely from theory, such as the total Z boson hadronic width [32], are in tension with the small value of α_s of the ABM11 and JR sets. This argument aside, the ABM11 set is not proven to be inconsistent with LHC data. We believe that we cannot disregard it for the crucial studies in the search of the Higgs boson.

One could attempt to enlarge further the pdf uncertainty that we have assigned to our benchmark MSTW08 set. Such a remedy is inadequate for the calculation of the likelihood of a Higgs boson mass hypothesis in LHC data. Uncertainties assigned to parton densities are typically treated as nuisance parameters in such a calculation. This can be largely justified by the fact that a significant component of the pdf uncertainty is due to statistical fluctuations of the measurements from which they are extracted. However, the discrepancy between ABM11 and MSTW08 is of a systematic nature. Given the large difference in central values, enlarging the statistical uncertainty of the MSTW08 set is equivalent to arbitrarily assigning a smaller weight to the ABM11 cross-section values.

Until a clearer theoretical understanding of the pdf discrepancies is available, we find it prudent to adopt the ABM11 set as our second benchmark set. In this publication, we provide tables of cross-section values for both the MSTW08 set and the ABM11 set. For the MSTW08 we quote the pdf uncertainty at the 90% CL. We use the ABM11 set (with 68% CL uncertainty) as a means to obtain a lower estimate of the cross-section.

4. Higgs boson width and signal-background interference

`iHixs` computes the partonic cross-section for resonant production and decay of a Higgs boson in the s -channel approximation, by performing an integration over the invariant mass of the Higgs decay products:

$$\hat{\sigma}_{ij \rightarrow \{H_{\text{final}}\}+X}(\hat{s}, \mu_f) = \int_{Q_a^2}^{Q_b^2} dQ^2 \frac{Q \Gamma_H(Q)}{\pi} \frac{\hat{\sigma}_{ij \rightarrow H}(\hat{s}, Q^2, \mu_f) \text{Br}_{H \rightarrow \{H_{\text{final}}\}}(Q)}{\Delta(Q, m_H)}. \quad (4.1)$$

The total cross-section corresponds to summing over all Higgs boson final states,

$$\sum_{\text{final}} \text{Br}_{H \rightarrow \{H_{\text{final}}\}}(Q) = 1. \quad (4.2)$$

The function Δ arises from s -channel Higgs propagator diagrams and it diverges at leading order in perturbation theory for $Q \rightarrow m_H$. A resummation of dominant Feynman diagrams in this limit at all orders in perturbation theory is necessary in order to obtain a sensible finite result.

`iHixs` permits an easy implementation of various schemes for the propagator function Δ . An optimal treatment of finite width effects is the subject of ongoing research. As a diagnostic of potentially sizable contributions we have employed the following schemes:

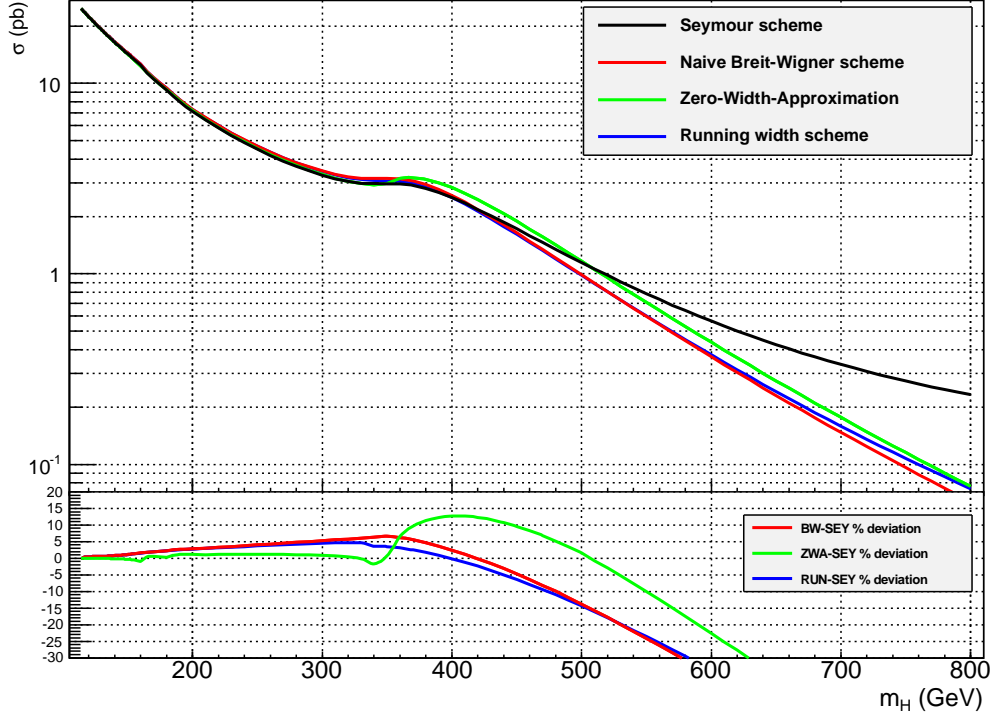


Figure 4: Inclusive Higgs cross-section at NNLO with various treatments of the Higgs propagator. The percentage difference with respect to the cross-section in the Seymour scheme is shown in the lower panel.

- **Zero width approximation (ZWA):**

$$\frac{1}{\Delta(Q, m_H)} \rightarrow \frac{\pi}{m_H \Gamma_H(m_H)} \delta(Q^2 - m_H^2) \quad (4.3)$$

This should be an adequate treatment for a light Higgs boson where the width of the Higgs boson is very small in comparison to its mass.

- **Naive Breit-Wigner (BW):**

$$\frac{1}{\Delta(Q, m_H)} = \frac{1}{(Q^2 - m_H^2)^2 + m_H^2 \Gamma_H^2(m_H)} \quad (4.4)$$

This corresponds to resumming leading width contributions for $Q \sim m_H$.

- **Breit-Wigner with running width:**

$$\frac{1}{\Delta(Q, m_H)} = \frac{1}{(Q^2 - m_H^2)^2 + Q^2 \Gamma_H^2(Q)} \quad (4.5)$$

We evaluate the width of the Higgs boson using HDECAY [19]. Our numerical results of Section 6 are obtained with this scheme.

- **Seymour scheme** [21]

$$\frac{1}{\Delta(Q, m_H)} = \frac{m_H^4/Q^4}{(Q^2 - m_H^2)^2 + \Gamma_H^2(m_H^2) \frac{Q^4}{m_H^2}} \quad (4.6)$$

This scheme is a prescription to account for signal-background interference effects at the high energy limit and finite width resummation simultaneously.

In Figure 4, we present the Higgs boson cross-section using the above treatments of Higgs width effects as a function of the Higgs boson mass. We notice that finite width and signal-background interference effects (as accounted for in the Seymour scheme [21]) become important for Higgs boson masses above 400 GeV. For such high values of the Higgs boson mass, where the width grows, the precise form of the Higgs propagator $\Delta(Q, m_H)$ is important and requires a consistent resummation of resonant diagrams. For a recent study we refer the reader to Ref. [22]. We emphasize that signal-background interference effects must always be accounted for by dedicated calculations such as in Refs [33–37].

5. Numerical estimates of the gluon fusion cross-section

In this Section, we present numerical results for the Higgs boson total cross-section at the LHC with 8 TeV energy and values of the Higgs boson mass in the range $m_H \in [114, 400]$ GeV. We treat finite width effects using the running width scheme of Section 4. We defer a detailed study of the case of a heavier Higgs boson for a future publication. As explained in Section 3 we present, in tables 1 and 2, results for two pdf benchmark sets: a representative set MSTW08 (with pdf uncertainties quoted at the 90% confidence level) and the ABM11 set which typically yields the smallest Higgs boson cross-sections (with pdf uncertainties quoted at the 68% confidence level). The predictions of these two sets are discrepant and we do not attempt to combine them in an “average” of any type.

We note that all of the results in this section can be reproduced with the publicly available program `iHixs`. The runcard options that we have used to obtain the central values of the cross-section predictions are:

<code>pdf_provider : {MSTW90,MSTW90_M,MSTW90_P,ABM}</code>	<code>K_ewk_real = 1.0</code>
<code>effective_theory_flag = 0</code>	<code>K_ewk_real_b = 1.0</code>
<code>no_error_flag = 0</code>	<code>m_top = 172.5</code>
<code>collider = LHC</code>	<code>Gamma_top = 0.0</code>
<code>Etot = 8000</code>	<code>Y_top = 1.0</code>
<code>higgs_width_scheme = 2</code>	<code>m_bot = 3.63</code>
<code>mhiggs : [114,400]</code>	<code>Gamma_bot = 0.0</code>
<code>muf/mhiggs : {0.5,0.25,1.0}</code>	<code>Y_bot = 1.0</code>
<code>mur/mhiggs : {0.5,0.25,1.0}</code>	<code>m_Z = 91.1876</code>
<code>DecayMode = total</code>	<code>Gamma_Z = 2.4952</code>
<code>ProductionMode = gg</code>	<code>m_W = 80.403</code>
<code>K_ewk = 1.0</code>	<code>Gamma_W = 2.141</code>

6. Summary

In this article, we have presented predictions for the inclusive gluon fusion cross-section at the LHC with 8 TeV center of mass energy using our publicly available program `iHixs` [5]. We have reviewed the perturbative convergence of the cross-section and derived uncertainty estimates due to uncalculated higher order effects by means of scale variations.

We have also reviewed the sensitivity of the cross-section on all available NNLO sets of parton distribution functions which are available through LHAPDF [26]. We have adopted the MSTW08 pdf set with uncertainties at the 90% confidence level as our representative benchmark. We have observed that the ABM11 pdf set typically yields the smallest cross-section values. We present the cross-section predictions with ABM11 which can be used for a more conservative estimate of the Higgs boson production rate.

We have studied the impact of finite width effects for large values of the Higgs boson mass. We limit our predictions to mass values where these effects can be neglected. The case of very heavy and very wide Higgs boson will be analyzed in a future publication.

We hope that our results will be a useful input for the experimental searches of the Higgs boson at the LHC in 2012.

Acknowledgments

Research supported by the Swiss National Foundation under contract SNF 200020-126632.

References

- [1] A. Collaboration, arXiv:1202.1408 [hep-ex].
- [2] S. Chatrchyan *et al.* [CMS Collaboration], arXiv:1202.1488 [hep-ex].
- [3] T. Aaltonen *et al.* [CDF and D0 Collaboration], arXiv:1103.3233 [hep-ex].
- [4] R. Barate *et al.* [LEP Working Group for Higgs boson searches and ALEPH Collaboration and and], Phys. Lett. B **565** (2003) 61 [arXiv:hep-ex/0306033].
- [5] C. Anastasiou, S. Buehler, F. Herzog and A. Lazopoulos, JHEP **1112** (2011) 058 [arXiv:1107.0683 [hep-ph]].
- [6] C. Anastasiou and K. Melnikov, Nucl. Phys. B **646**, 220 (2002) [arXiv:hep-ph/0207004].
- [7] C. Anastasiou, S. Beerli, S. Bucherer, A. Daleo and Z. Kunszt, JHEP **0701** (2007) 082 [arXiv:hep-ph/0611236].
- [8] C. Anastasiou, S. Bucherer and Z. Kunszt, JHEP **0910**, 068 (2009) [arXiv:0907.2362 [hep-ph]].
- [9] E. Furlan, JHEP **1110** (2011) 115 [arXiv:1106.4024 [hep-ph]].
- [10] S. Buehler and C. Duhr, arXiv:1106.5739 [hep-ph].
- [11] U. Aglietti, R. Bonciani, G. Degrossi and A. Vicini, Phys. Lett. B **595**, 432 (2004) [arXiv:hep-ph/0404071].
- [12] C. Anastasiou, R. Boughezal and F. Petriello, JHEP **0904**, 003 (2009) [arXiv:0811.3458 [hep-ph]].
- [13] S. Actis, G. Passarino, C. Sturm and S. Uccirati, Phys. Lett. B **670**, 12 (2008) [arXiv:0809.1301 [hep-ph]].
- [14] A. van Hameren, arXiv:1007.4716 [hep-ph].
- [15] R. K. Ellis and G. Zanderighi, JHEP **0802** (2008) 002 [arXiv:0712.1851 [hep-ph]].
- [16] T. Hahn, Comput. Phys. Commun. **168** (2005) 78 [arXiv:hep-ph/0404043].
- [17] M. R. Whalley, D. Bourilkov and R. C. Group, arXiv:hep-ph/0508110.
- [18] R. V. Harlander and W. B. Kilgore, Phys. Rev. Lett. **88**, 201801 (2002) [arXiv:hep-ph/0201206].
- [19] A. Djouadi, J. Kalinowski and M. Spira, Comput. Phys. Commun. **108** (1998) 56 [arXiv:hep-ph/9704448].
- [20] V. Ravindran, J. Smith and W. L. van Neerven, Nucl. Phys. B **665**, 325 (2003) [arXiv:hep-ph/0302135]. R. V. Harlander, W. B. Kilgore, Phys. Rev. **D68**, 013001 (2003). [hep-ph/0304035]. D. Graudenz, M. Spira and P. M. Zerwas, Phys. Rev. Lett. **70** (1993) 1372. M. Spira, A. Djouadi, D. Graudenz and P. M. Zerwas, Nucl. Phys. B **453**, 17 (1995) [arXiv:hep-ph/9504378]. S. Dawson, Nucl. Phys. B **359**, 283 (1991). A. Djouadi, M. Spira and P. M. Zerwas, Phys. Lett. B **264** (1991) 440. R. Harlander and P. Kant, JHEP **0512**, 015 (2005) [arXiv:hep-ph/0509189]. U. Aglietti, R. Bonciani, G. Degrossi and A. Vicini, JHEP **0701**, 021 (2007) [arXiv:hep-ph/0611266]. U. Baur and E. W. N. Glover, Nucl. Phys. B **339**, 38 (1990). R. Bonciani, G. Degrossi and A. Vicini, JHEP **0711**, 095 (2007) [arXiv:0709.4227 [hep-ph]]. C. Anastasiou, R. Boughezal and E. Furlan, JHEP **1006**, 101 (2010)

- [arXiv:1003.4677 [hep-ph]]. K. G. Chetyrkin, B. A. Kniehl and M. Steinhauser, Phys. Rev. Lett. **79** (1997) 353 [arXiv:hep-ph/9705240]. M. Kramer, E. Laenen and M. Spira, Nucl. Phys. B **511** (1998) 523 [arXiv:hep-ph/9611272]. S. Actis, G. Passarino, C. Sturm and S. Uccirati, Nucl. Phys. B **811**, 182 (2009) [arXiv:0809.3667 [hep-ph]]. W. Y. Keung and F. J. Petriello, Phys. Rev. D **80**, 013007 (2009) [arXiv:0905.2775 [hep-ph]]. A. van Hameren, C. G. Papadopoulos and R. Pittau, JHEP **0909** (2009) 106 [arXiv:0903.4665 [hep-ph]].
- [21] M. H. Seymour, Phys. Lett. B **354**, 409 (1995) [hep-ph/9505211].
- [22] S. Gorla, G. Passarino and D. Rosco, arXiv:1112.5517 [hep-ph].
- [23] D. de Florian and M. Grazzini, Phys. Lett. B **674** (2009) 291 [arXiv:0901.2427 [hep-ph]].
- [24] V. Ahrens, T. Becher, M. Neubert and L. L. Yang, Phys. Lett. B **698** (2011) 271 [arXiv:1008.3162 [hep-ph]].
- [25] S. Moch and A. Vogt, Phys. Lett. B **631** (2005) 48 [arXiv:hep-ph/0508265].
- [26] <http://hepforge.cedar.ac.uk/lhapdf/>
- [27] A. D. Martin, W. J. Stirling, R. S. Thorne and G. Watt, Eur. Phys. J. C **63** (2009) 189 [arXiv:0901.0002 [hep-ph]].
- [28] P. Jimenez-Delgado and E. Reya, Phys. Rev. D **80** (2009) 114011 [arXiv:0909.1711 [hep-ph]].
- [29] R. D. Ball *et al.* [The NNPDF Collaboration], Nucl. Phys. B **855** (2012) 153 [arXiv:1107.2652 [hep-ph]].
- [30] S. Alekhin, J. Blumlein and S. Moch, arXiv:1202.2281 [hep-ph].
- [31] S. Bethke, Eur. Phys. J. C **64** (2009) 689 [arXiv:0908.1135 [hep-ph]].
- [32] P. A. Baikov, K. G. Chetyrkin, J. H. Kuhn and J. Rittinger, arXiv:1201.5804 [hep-ph].
- [33] L. J. Dixon and M. S. Siu, Phys. Rev. Lett. **90** (2003) 252001 [hep-ph/0302233].
- [34] L. J. Dixon and Y. Sofianatos, Phys. Rev. D **79** (2009) 033002 [arXiv:0812.3712 [hep-ph]].
- [35] M. Dührssen, K. Jakobs, J. J. van der Bij and P. Marquard, JHEP **0505**, 064 (2005) [hep-ph/0504006].
- [36] T. Binoth, M. Ciccolini, N. Kauer and M. Kramer, JHEP **0612** (2006) 046 [hep-ph/0611170].
- [37] J. M. Campbell, R. K. Ellis and C. Williams, JHEP **1110** (2011) 005 [arXiv:1107.5569 [hep-ph]].

$m_H(\text{GeV})$	MSTW08 $\sigma(pb)$	$\% \delta_{PDF}$	$\% \delta_{\mu_F}$	ABM11 $\sigma(pb)$	$\% \delta_{PDF}$	$\% \delta_{\mu_F}$
114	24.69	+7.92 -7.54	+8.83 -9.32	22.78	+2.28 -2.28	+8.0 -8.85
115	24.27	+7.91 -7.54	+9.07 -9.31	22.38	+2.29 -2.29	+7.98 -8.84
116	23.94	+7.9 -7.61	+8.75 -9.59	22.0	+2.29 -2.29	+8.0 -8.83
117	23.55	+7.93 -7.54	+8.64 -9.33	21.68	+2.29 -2.29	+7.92 -9.05
118	23.17	+7.92 -7.54	+8.6 -9.38	21.33	+2.3 -2.3	+7.84 -8.84
119	22.79	+7.92 -7.53	+8.55 -9.35	20.98	+2.3 -2.3	+7.79 -8.87
120	22.42	+7.91 -7.53	+8.53 -9.3	20.63	+2.3 -2.3	+7.77 -8.85
121	22.06	+7.91 -7.53	+8.51 -9.34	20.29	+2.3 -2.3	+7.75 -8.82
122	21.7	+7.91 -7.53	+8.47 -9.28	19.96	+2.31 -2.31	+7.74 -8.82
123	21.36	+7.8 -7.53	+8.42 -9.28	19.64	+2.31 -2.31	+7.72 -8.86
124	21.02	+7.81 -7.52	+8.41 -9.25	19.32	+2.31 -2.31	+7.68 -8.81
125	20.69	+7.79 -7.53	+8.37 -9.26	19.01	+2.32 -2.32	+7.65 -8.82
126	20.37	+7.8 -7.53	+8.35 -9.24	18.71	+2.32 -2.32	+7.64 -8.8
127	20.05	+7.8 -7.52	+8.34 -9.21	18.41	+2.32 -2.32	+7.6 -8.84
128	19.74	+7.79 -7.52	+8.3 -9.2	18.13	+2.33 -2.33	+7.58 -8.79
129	19.44	+7.8 -7.52	+8.28 -9.26	17.84	+2.33 -2.33	+7.56 -8.79
130	19.14	+7.79 -7.51	+8.24 -9.19	17.57	+2.33 -2.33	+7.54 -8.84
131	18.86	+7.8 -7.51	+8.22 -9.17	17.3	+2.34 -2.34	+7.51 -8.79
132	18.57	+7.79 -7.51	+8.19 -9.16	17.03	+2.34 -2.34	+7.47 -8.77
133	18.3	+7.8 -7.5	+8.17 -9.15	16.77	+2.35 -2.35	+7.46 -8.75
134	18.03	+7.79 -7.51	+8.14 -9.15	16.52	+2.35 -2.35	+7.41 -8.74
135	17.76	+7.8 -7.51	+8.12 -9.19	16.27	+2.35 -2.35	+7.39 -8.73
136	17.5	+7.8 -7.5	+8.05 -9.17	16.03	+2.36 -2.36	+7.37 -8.73
137	17.25	+7.78 -7.53	+8.05 -9.17	15.79	+2.36 -2.36	+7.36 -8.75
138	17.01	+7.79 -7.51	+8.01 -9.13	15.56	+2.37 -2.37	+7.31 -8.73
139	16.77	+7.8 -7.51	+7.97 -9.08	15.34	+2.37 -2.37	+7.26 -8.7
140	16.53	+7.79 -7.5	+7.9 -9.06	15.12	+2.37 -2.37	+7.24 -8.69
141	16.3	+7.79 -7.5	+7.88 -9.03	14.9	+2.38 -2.38	+7.23 -8.67
142	16.07	+7.79 -7.5	+7.87 -9.01	14.69	+2.38 -2.38	+7.2 -8.62
143	15.85	+7.78 -7.51	+7.85 -9.0	14.48	+2.39 -2.39	+7.19 -8.62
144	15.64	+7.78 -7.5	+7.82 -8.99	14.28	+2.39 -2.39	+7.18 -8.62
145	15.43	+7.78 -7.51	+7.79 -8.99	14.08	+2.4 -2.4	+7.16 -8.6
146	15.22	+7.79 -7.51	+7.78 -8.97	13.88	+2.4 -2.4	+7.18 -8.57
147	15.02	+7.79 -7.5	+7.74 -8.97	13.69	+2.41 -2.41	+7.14 -8.59
148	14.81	+7.8 -7.51	+7.74 -8.97	13.5	+2.41 -2.41	+7.12 -8.58
149	14.62	+7.8 -7.5	+7.74 -8.93	13.32	+2.42 -2.42	+7.1 -8.57
150	14.43	+7.78 -7.51	+7.7 -8.93	13.14	+2.42 -2.42	+7.08 -8.55

Table 1: Inclusive Higgs production cross-section through gluon fusion (in pb) at $\sqrt{s} = 8$ TeV, with pdf and scale uncertainties for the MSTW08 and ABM11 pdf sets. The pdf uncertainty for MSTW08 is calculated using the 90%CL grids, for reasons explained in section 3, while the ABM11 uncertainty corresponds to 68%CL.

$m_H(\text{GeV})$	MSTW08 $\sigma(pb)$	$\% \delta_{PDF}$	$\% \delta_{\mu_F}$	ABM11 $\sigma(pb)$	$\% \delta_{PDF}$	$\% \delta_{\mu_F}$
151	14.24	+7.79 -7.52	+7.67 -8.95	12.97	+2.43 -2.43	+7.04 -8.61
152	14.06	+7.78 -7.52	+7.62 -9.01	12.8	+2.43 -2.43	+7.02 -8.62
153	13.88	+7.8 -7.52	+7.61 -8.99	12.63	+2.44 -2.44	+7.0 -8.62
154	13.71	+7.8 -7.52	+7.6 -8.99	12.46	+2.44 -2.44	+6.99 -8.6
155	13.53	+7.8 -7.51	+7.58 -8.96	12.3	+2.45 -2.45	+6.98 -8.59
160	12.66	+7.81 -7.51	+7.5 -8.9	11.48	+2.48 -2.48	+6.91 -8.55
165	11.56	+7.81 -7.54	+7.39 -8.87	10.47	+2.5 -2.5	+6.81 -8.53
170	10.72	+7.83 -7.55	+7.26 -8.86	9.68	+2.53 -2.53	+6.7 -8.52
175	10.03	+7.84 -7.56	+7.17 -8.83	9.05	+2.57 -2.57	+6.64 -8.49
180	9.42	+7.85 -7.58	+7.08 -8.81	8.47	+2.6 -2.6	+6.57 -8.47
185	8.77	+7.87 -7.59	+7.0 -8.78	7.88	+2.63 -2.63	+6.49 -8.46
190	8.21	+7.87 -7.62	+6.91 -8.76	7.36	+2.66 -2.66	+6.42 -8.45
195	7.74	+7.9 -7.64	+6.83 -8.73	6.92	+2.7 -2.7	+6.33 -8.43
200	7.32	+7.91 -7.66	+6.76 -8.7	6.53	+2.73 -2.73	+6.26 -8.41
210	6.6	+7.95 -7.71	+6.58 -8.65	5.86	+2.8 -2.8	+6.14 -8.36
220	6.0	+7.98 -7.76	+6.42 -8.6	5.3	+2.87 -2.87	+6.01 -8.32
230	5.49	+8.02 -7.78	+6.28 -8.54	4.83	+2.95 -2.95	+5.87 -8.29
240	5.05	+8.07 -7.89	+6.14 -8.47	4.42	+3.03 -3.03	+5.76 -8.24
250	4.67	+8.11 -7.9	+6.0 -8.41	4.07	+3.1 -3.1	+5.65 -8.17
260	4.34	+8.15 -8.01	+5.84 -8.34	3.77	+3.19 -3.19	+5.52 -8.11
270	4.06	+8.2 -8.04	+5.68 -8.28	3.51	+3.27 -3.27	+5.37 -8.06
280	3.82	+8.25 -8.15	+5.52 -8.21	3.29	+3.35 -3.35	+5.23 -8.0
290	3.62	+8.41 -8.16	+5.34 -8.13	3.09	+3.43 -3.43	+5.07 -7.94
300	3.45	+8.46 -8.28	+5.14 -8.05	2.93	+3.51 -3.51	+4.89 -7.85
310	3.3	+8.51 -8.29	+4.92 -7.93	2.8	+3.6 -3.6	+4.69 -7.76
320	3.2	+8.55 -8.41	+4.65 -7.81	2.69	+3.68 -3.68	+4.45 -7.64
330	3.13	+8.6 -8.42	+4.31 -7.65	2.62	+3.76 -3.76	+4.12 -7.49
340	3.09	+8.65 -8.53	+3.87 -7.43	2.58	+3.84 -3.84	+3.69 -7.28
350	3.07	+8.71 -8.55	+3.74 -7.37	2.55	+3.92 -3.92	+3.59 -7.22
360	3.06	+8.75 -8.57	+4.13 -7.63	2.53	+4.0 -4.0	+4.03 -7.46
370	2.99	+8.81 -8.69	+4.46 -7.79	2.46	+4.08 -4.08	+4.37 -7.64
380	2.86	+8.86 -8.71	+4.65 -7.89	2.34	+4.16 -4.16	+4.58 -7.75
390	2.69	+9.03 -8.82	+4.73 -7.92	2.2	+4.24 -4.24	+4.67 -7.77
400	2.51	+9.08 -8.83	+4.73 -7.91	2.04	+4.32 -4.32	+4.67 -7.78

Table 2: Inclusive Higgs production cross-section through gluon fusion (in pb) at $\sqrt{s} = 8$ TeV, with pdf and scale uncertainties for the MSTW08 and ABM11 pdf sets. The pdf uncertainty for MSTW08 is calculated using the 90%CL grids, for reasons explained in section 3, while the ABM11 uncertainty corresponds to 68%CL.